



Cite this: *Chem. Commun.*, 2015,  
51, 10879

Received 24th April 2015,  
Accepted 27th May 2015

DOI: 10.1039/c5cc03428k

[www.rsc.org/chemcomm](http://www.rsc.org/chemcomm)

## Quantitative determination of fluoride in pure water using luminescent europium complexes<sup>†</sup>

Stephen J. Butler

Two luminescent probes  $[\text{Eu}.\text{L}^{1-2}]^+$  are reported for the rapid detection of fluoride in water. Probes  $[\text{Eu}.\text{L}^{1-2}]^+$  exhibit exceptional enhancements in Eu emission in the presence of fluoride, permitting its selective determination within the environmentally relevant concentration range (20–210  $\mu\text{M}$ ).

Fluoride is considered essential for healthy teeth and bone growth; in several countries this has led to the artificial fluoridation of water supplies. Fluoride is also introduced into water supplies through the production of phosphate containing fertilizers and aluminium processing industries. Consumption of elevated levels of fluoride in drinking water can cause dental and skeletal fluorosis, as well as acute gastric problems and kidney failure. Therefore, controlling the level of fluoride in water supplies is a global governmental concern; the maximum recommended concentration of fluoride in drinking water defined by the World Health Organization guidelines is 4 mg  $\text{L}^{-1}$ , or 210  $\mu\text{M}$ . Consequently, the development of convenient analytical methods for the rapid, quantitative detection of fluoride in water samples has become an active area of research.

Traditional methods for the accurate analysis of fluoride involve the use of ion-selective electrodes and ion chromatography. However, such approaches can be time-consuming, require expensive instrumentation and are not practical for measuring fluoride concentrations *in vivo*. In recent years, a number of alternative strategies have been devised, such as the development of colorimetric or luminescent molecular probes, and reaction-based (irreversible) chemodosimeters.<sup>1–6</sup> The creation of probes for fluoride recognition in water is particularly challenging because of the high free energy of hydration of fluoride ( $-\Delta G_{\text{hyd}}^\circ = 465 \text{ kJ mol}^{-1}$ ) compared to other anions, together with its relatively small ionic radius (1.26 Å). Most probes reported to date have been limited in sensing

applications, because they suffer from interference from other anions present in water samples (e.g. chloride, nitrate, sulfate and phosphate) that bind competitively. Furthermore, very few probes can actually detect fluoride ions in a pure aqueous medium;<sup>1</sup> the majority of reported systems are restricted for use in organic solvents such as acetonitrile,<sup>2</sup> DMSO,<sup>3</sup> methanol<sup>4</sup> or dichloromethane,<sup>5</sup> or they require a solvent mixture of organic solvent and water.<sup>6</sup> Reaction-based probes, such as those which rely on fluoride-mediated cleavage of a Si–O bond, are irreversible and typically suffer from delayed acquisition times (10 min to several hours).<sup>1b,d</sup>

Over the last decade, several emissive lanthanide (Ln) complexes have been developed that can report changes in the concentrations of various anions, including citrate, lactate and bicarbonate, through modulation of emission spectral form or lifetime of the complex.<sup>7,8</sup> However, Ln-based sensors for fluoride are scarce because the binding affinity between fluoride and Ln ions is generally too weak ( $\log K_a = 1.5–3$ ).<sup>8c,9</sup> One notable example involved the encapsulation of fluoride between two Eu complexes, resulting in a supramolecular dimer ( $\log \beta = 13.0$ ).<sup>1e</sup> In this case, the fluoride detection range was very low (0.2–50  $\mu\text{M}$ ), falling outside of the environmentally significant range (20–210  $\mu\text{M}$ ).

In this work, two water-soluble luminescent probes  $[\text{Eu}.\text{L}^{1-2}]^+$  are reported (Fig. 1), each capable of binding and sensing fluoride in pure water samples, with minimal interference from other anions. Each probe is based on a  $C_2$ -symmetric mono-cationic europium complex, bearing two *trans*-related quinoline chromophores and a coordinated water molecule. Fluoride binds reversibly to each probe, displacing the coordinated water, resulting in a 9-fold enhancement in the overall emission intensity and

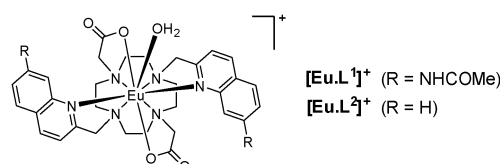


Fig. 1 Structure of luminescent europium complexes  $[\text{Eu}.\text{L}^{1-2}]^+$ .

Department of Chemistry, Loughborough University, Leicestershire, LE11 3TU, UK.  
 E-mail: [s.j.butler@lboro.ac.uk](mailto:s.j.butler@lboro.ac.uk)

<sup>†</sup> Electronic supplementary information (ESI) available: Details of complex synthesis and characterization, and UV-Vis, fluorescence and NMR spectral data are available. See DOI: 10.1039/c5cc03428k



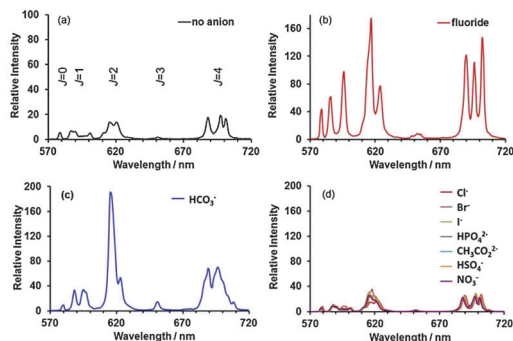


Fig. 2 Comparison of the emission spectrum of (a)  $[\text{Eu}.\text{L}^1]^+$  with the limiting emission spectra of  $[\text{Eu}.\text{L}^1]^+$  in the presence of: (b) 2 mM fluoride; (c) 2 mM  $\text{HCO}_3^-$ ; and (d) 2 mM  $\text{Cl}^-$ ,  $\text{Br}^-$ ,  $\text{I}^-$ ,  $\text{HPO}_4^{2-}$ ,  $\text{CH}_3\text{COO}^-$ ,  $\text{HSO}_4^-$ ,  $\text{NO}_3^-$  (sodium salts). Conditions:  $\text{H}_2\text{O}$  (25 mM HEPES, pH 7.4),  $\lambda_{\text{exc}} = 332$  nm, 298 K.

Table 1 Selected photophysical data for Eu complexes  $[\text{Eu}.\text{L}^{1-2}]^+$  ( $\text{H}_2\text{O}$ , or as stated)

Complex	$\lambda_{\text{max}}/\text{nm}$	$\epsilon/\text{mM}^{-1} \text{ cm}^{-1}$	$\phi_{\text{em}}/\%$ <sup>a</sup>	$\tau_{(\text{H}_2\text{O})}/\text{ms}$	$\tau_{(\text{D}_2\text{O})}/\text{ms}$	$q$ <sup>b</sup>
$[\text{Eu}.\text{L}^1]^+$	332	12.5	7	0.49	1.38	1.2
$[\text{Eu}.\text{L}^2]^+$	318	11.8	23	0.51	1.37	1.1

<sup>a</sup> Errors on quantum yields and lifetimes are  $\pm 15\%$ . <sup>b</sup> Values of hydration state,  $q$  ( $\pm 20\%$ ) are derived using methods in ref. 10.

dramatic changes in emission spectral form (Fig. 2). Complex  $[\text{Eu}.\text{L}^1]^+$  represents one of the very few probes capable of signalling the presence of fluoride within the range relevant to water fluoridation (20–210  $\mu\text{M}$ ),<sup>1a,d</sup> and provides an instantaneous spectral readout signal.

Details of the synthesis of complexes  $[\text{Eu}.\text{L}^{1-2}]^+$  are provided in the ESI.† Selected photophysical data for  $[\text{Eu}.\text{L}^{1-2}]^+$  are provided in Table 1. The UV-Vis absorption spectrum of  $[\text{Eu}.\text{L}^1]^+$  is composed of a broad featureless band centred at 332 nm, whereas the absorption spectrum of  $[\text{Eu}.\text{L}^2]^+$  features a narrow band with a maximum at 318 nm (Fig. S1 and S2, ESI†). The emission spectra of  $[\text{Eu}.\text{L}^{1-2}]^+$  in water (25 mM HEPES, pH 7.4) were similar, each characterised by at least three components in the  $\Delta J = 1$  transition (585–605 nm), indicating that both complexes adopt structures of low symmetry in water (Fig. 2a). In addition, the  $\Delta J = 2$  transition (605–625 nm) is approximately equal in intensity to the  $\Delta J = 4$  manifold (685–710 nm).

To assess the ability of  $[\text{Eu}.\text{L}^{1-2}]^+$  to signal the presence of different anions, the emission spectrum of  $[\text{Eu}.\text{L}^1]^+$  (20  $\mu\text{M}$ ) was recorded in water (25 mM HEPES, pH 7.4) in the presence of a 100-fold excess of a range of anions (Fig. 2). The addition of fluoride resulted in a 9-fold enhancement in the overall emission intensity of  $[\text{Eu}.\text{L}^1]^+$ , as well as substantial perturbations in the emission spectral form (Fig. 2b). The limiting spectrum indicated the formation of one major fluoride-bound species, as defined by a single  $\Delta J = 0$  transition at 579 nm and two intense components within the  $\Delta J = 1$  transition, centred at 586 and 596 nm respectively. In addition, the relative intensity of the hypersensitive  $\Delta J = 2$  transition centred at 617 nm increased by a factor of 15. The only other anion that induced a significant

spectral response was bicarbonate. In the presence of  $\text{HCO}_3^-$ , the limiting spectrum of  $[\text{Eu}.\text{L}^1]^+$  (Fig. 2c) was distinctly different from that observed with fluoride. Most notably, a larger ratio between the transitions  $\Delta J = 2/\Delta J = 1$  was observed. In contrast, all other anions typically present in water samples, including chloride, phosphate, sulfate and nitrate induced essentially no change ( $< 10\%$ ) in emission intensity or spectral form (Fig. 2d). Complex  $[\text{Eu}.\text{L}^2]^+$  also showed a selective spectral response to fluoride, giving rise to a smaller (3.5-fold) enhancement in the overall emission intensity (Fig. S6, ESI†).

Emission lifetimes of  $[\text{Eu}.\text{L}^1]^+$  were measured in  $\text{H}_2\text{O}$  and  $\text{D}_2\text{O}$  in the presence of fluoride and were found to be similar ( $\tau = 1.13$  and 1.67 ms respectively), compared to those measured in the absence of a coordinating anion ( $\tau = 0.49$  and 1.38 ms). These results are consistent with a hydration state,  $q$ , of 1.2 ( $\pm 20\%$ ) in the absence of fluoride, and zero for the fluoride-bound species.<sup>10</sup> Thus, added fluoride results in displacement of the coordinated water molecule from the probe. The addition of  $\text{HCO}_3^-$  resulted in a similar change in the hydration state, whereas all other anions (e.g.  $\text{Cl}^-$ ,  $\text{Br}^-$ ,  $\text{I}^-$ ,  $\text{HPO}_4^{2-}$ ,  $\text{CH}_3\text{COO}^-$ ,  $\text{HSO}_4^-$ ,  $\text{NO}_3^-$ ) did not displace the bound water molecule. A 1:1 binding mode between  $[\text{Eu}.\text{L}^1]^+$  and fluoride was confirmed by high resolution mass spectrometric data; a major signal was observed at  $m/z = 875.2302$  for the singly charged ternary complex  $^{151}\text{Eu}.\text{L}^1 + \text{F} + \text{Na}^+$ , in excellent agreement with the calculated isotopic distribution (Fig. S13, ESI†).

An affinity constant was determined for fluoride binding by making incremental additions of NaF to a solution of  $[\text{Eu}.\text{L}^1]^+$  (20  $\mu\text{M}$ ) at pH 7.4 (25 mM HEPES). The change in the emission intensity ratio, 596/615 nm, was measured as a function of anion concentration, and the data were analysed using a non-linear least squares curve-fitting procedure based on a 1:1 binding model (Fig. S4 and S5, ESI†).  $[\text{Eu}.\text{L}^1]^+$  was found to bind to fluoride with  $\log K_a = 3.5 (\pm 0.1)$ . Under the same conditions,  $[\text{Eu}.\text{L}^2]^+$  showed a slightly weaker affinity for bicarbonate [ $\log K_a = 3.0 (\pm 0.1)$ ]. To eliminate competitive binding to  $\text{HCO}_3^-$  entirely, a fluoride titration experiment was conducted at pH 6 using 25 mM MES buffer (at pH 6, residual  $\text{HCO}_3^-$  is readily removed as  $\text{CO}_2$ ) (Fig. 3).<sup>11</sup> Under these conditions, an affinity

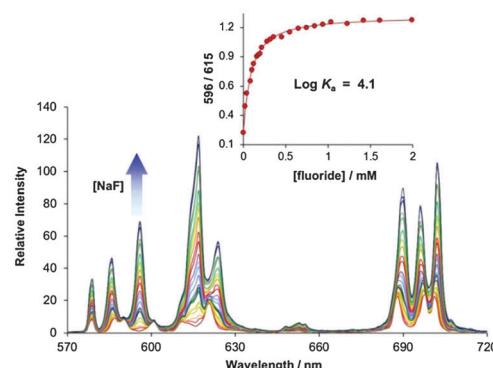


Fig. 3 Change in emission spectra of  $[\text{Eu}.\text{L}^1]^+$  (20  $\mu\text{M}$ ) as a function of added NaF. Conditions:  $\text{H}_2\text{O}$  (25 mM MES, pH 6.0),  $\lambda_{\text{exc}} = 332$  nm, 298 K. The inset shows the fit to the experimental data, for  $\log K_a = 4.1 (\pm 0.1)$ .



constant for the binding of fluoride to  $[\text{Eu.L}^1]^+$  was  $\log K_a = 4.1 (\pm 0.1)$ . This is 5 times stronger than that determined at pH 7.4, reflecting the absence of  $\text{HCO}_3^-$  at lower pH. Complex  $[\text{Eu.L}^2]^+$ , which lacks acetamide groups, showed slightly weaker binding to fluoride ( $\log K_a = 3.5 \pm 0.1$ ) under the same conditions.

The affinity of  $[\text{Eu.L}^{1-2}]^+$  for fluoride is substantially higher than that of previously reported Ln-F systems. This can be ascribed to a synergistic effect between Eu(III) coordination and additional hydrogen bonding interactions to the electron deficient quinoline units. A molecular model of  $[\text{Eu.L}^2]^+$  with a coordinated fluoride ion [optimised at B3LYP/3-21G\* with the Gaussian 09 package, using water as solvent]<sup>12</sup> indicated that the bound fluoride can form two short C-H $\cdots$ F $^-$  contacts with each of the quinoline units (Fig. 4). The average C-H $\cdots$ F $^-$  distance is 2.81 Å, with an average H $\cdots$ F $^-$  distance of 1.88 Å. Both C-H $\cdots$ F $^-$  angles are acceptably linear (avg. angle is 141°).<sup>13</sup> It is hypothesised that these bifurcated C-H $\cdots$ F $^-$  $\cdots$ H-C contacts significantly stabilise the metal-bound fluoride. Such interactions would also restrict rotation of the quinoline N-Eu bonds, thus stabilising a single diastereomer, consistent with that observed in the Eu emission spectrum.

The dramatic changes in Eu emission spectral form of  $[\text{Eu.L}^{1-2}]^+$  observed in the presence of fluoride are indicative of alteration of the Eu(III) metal coordination environment. To probe this change further, the effect of fluoride on the  $^1\text{H}$  NMR spectrum of  $[\text{Eu.L}^1]^+$  was investigated in  $\text{D}_2\text{O}$  (pD 6.4). In the absence of added fluoride, two sets of proton resonances were clearly discernible in the  $^1\text{H}$  NMR spectrum of  $[\text{Eu.L}^1]^+$ ,

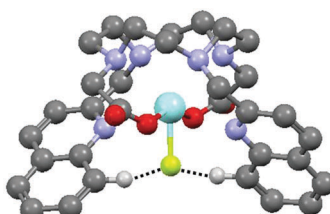


Fig. 4 An optimised structure of  $[\text{Eu.L}^2]^+$  with a coordinated fluoride ion, stabilised by two short C-H $\cdots$ F $^-$  contacts (avg. C-H $\cdots$ F $^-$  distance is 2.81 Å, avg. C-H $\cdots$ F $^-$  angle is 141°). The model geometry was optimised at B3LYP/3-21G\* (Gaussian 09 package) using the crystal structure of an Eu complex reported in ref. 14 as a starting point.

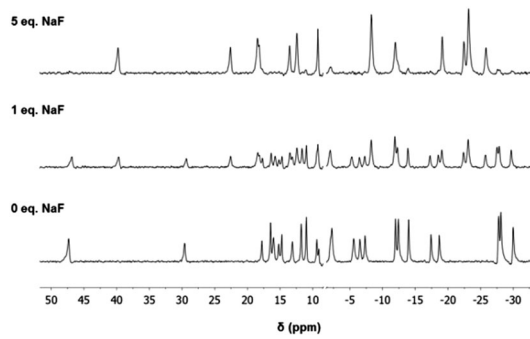


Fig. 5  $^1\text{H}$  NMR spectra of  $[\text{Eu.L}^1]^+$  (2.4 mM) upon addition of NaF (0–5 eq.). Measured in  $\text{D}_2\text{O}$  (pD 6.4, 298 K).

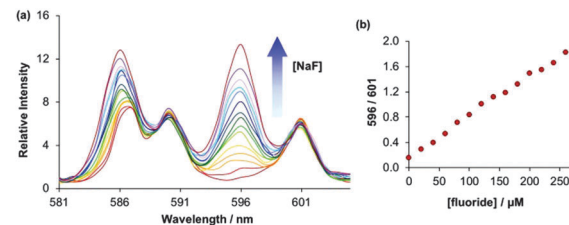


Fig. 6 (a) Ratiometric change in emission spectral form of  $[\text{Eu.L}^1]^+$  (20  $\mu\text{M}$ ) within the  $\Delta J = 1$  manifold (580–605 nm), as a function of added NaF (0–260  $\mu\text{M}$ ). (b) Linear increase in the emission intensity ratio, 596/601 nm, in the range relevant to water fluoridation. Conditions:  $\text{H}_2\text{O}$  (25 mM MES, pH 6.0),  $\lambda_{\text{exc}} = 332$  nm, 25 °C.

consistent with the presence of two diastereomers in solution (Fig. 5). The addition of 1 eq. of NaF resulted in the appearance of a new set of resonances corresponding to the fluoride-bound species, in slow exchange with the original hydrated complex on the NMR timescale. In the presence of excess NaF (5 eq.), the original signals disappeared and only signals for the fluoride-bound complex remained. The number of apparent signals has halved compared to the hydrated complex, indicating that a single fluoride-bound species has formed. Coordination of fluoride was also observed in the  $^{19}\text{F}$  NMR spectra, which showed a resonance at  $-123$  ppm for unbound fluoride, and the emergence of a second signal at  $-474$  ppm, corresponding to fluoride bound at the Eu metal centre (Fig. S11, ESI $^\ddagger$ ).

The remarkable sensitivity of the probe was demonstrated by plotting the emission intensity ratio, 596/601 nm, as a function of added NaF in the concentration range 0–260  $\mu\text{M}$  (Fig. 6). The plot showed very good linearity ( $R^2 = 0.9949$ ) within this range. Notably, a 200% enhancement in the intensity ratio was obtained after the addition of 260  $\mu\text{M}$  NaF. Competitive binding studies revealed that  $[\text{Eu.L}^{1-2}]^+$  can detect low micromolar levels of fluoride with essentially no interference from other anions typically found in drinking water (e.g.  $\text{Cl}^-$ ,  $\text{HPO}_4^{2-}$ ,  $\text{NO}_3^-$  and  $\text{SO}_4^{2-}$ ), even when present in high concentrations (5 mM) (Fig. S9, ESI $^\ddagger$ ). Thus,  $[\text{Eu.L}^1]^+$  represents one of the most sensitive probes for the selective determination of fluoride levels in drinking water.

To validate the practicable utility of probe  $[\text{Eu.L}^1]^+$ , tap water samples buffered at pH 6 (25 mM MES) were spiked with known concentrations of NaF. The amount of fluoride was measured by comparing the recorded emission spectra with the calibration curve in Fig. 6 (Table 2). The results obtained using  $[\text{Eu.L}^1]^+$

Table 2 Measurement of fluoride ion concentration in spiked tap water samples, using  $[\text{Eu.L}^1]^+$  and a fluoride-selective electrode (FSE)

Spiked $[\text{F}^-]/\mu\text{M}$	$[\text{F}^-]/\mu\text{M}$		$[\text{F}^-]/\mu\text{M}$ Using FSE $^\ddagger$
	Using $[\text{Eu.L}^1]^+$ $^\alpha$	% Variation $^\beta$	
30	36 ( $\pm 6$ )	3.0	35 ( $\pm 3$ )
65	65 ( $\pm 4$ )	7.0	68 ( $\pm 3$ )
115	113 ( $\pm 4$ )	6.0	111 ( $\pm 4$ )
160	154 ( $\pm 6$ )	6.5	165 ( $\pm 4$ )
210	204 ( $\pm 8$ )	5.0	212 ( $\pm 4$ )

$^\alpha$  Values are the mean average of two independent measurements.

$^\beta$  Calculated based on an initial  $\text{F}^-$  ion concentration of 5  $\mu\text{M}$ .



were in close agreement with the expected fluoride levels, with a maximal percentage variation of 7%. The results were also compared to those obtained independently using a fluoride-selective electrode (FSE); both analytical methods showed very good agreement.

In summary, two luminescent europium complexes  $[\text{Eu}(\text{L}^{1-2})]^+$  have been synthesised, each capable of selective binding to fluoride in water in the 20–260  $\mu\text{M}$  range. Such strong binding to fluoride can be attributed to a synergistic effect between Eu metal coordination and two stabilising  $\text{C}-\text{H}\cdots\text{F}^-$  interactions.  $[\text{Eu}(\text{L}^1)]^+$  was used for the quantitative determination of fluoride ions in drinking water samples, within the range relevant to water fluoridation (20–210  $\mu\text{M}$ ). These results establish Eu complexes as effective probes for fluoride analysis, offering advantages over traditional methods, including a rapid spectral readout signal. In addition, the ligand structure can be readily modified to modulate the steric demand at the Eu(III) metal centre, thus tuning anion affinity to the target concentration range.

SJB wishes to thank the Ramsay Memorial Fellowship Trust for funding, Dr Alan Kenwright and Dr Nicola Rodgers for help with NMR studies and Dr Mark Fox for molecular modelling studies.

## References

- (a) R. Hu, J. Feng, D. Hu, S. Wang, S. Li, Y. Li and G. Yang, *Angew. Chem., Int. Ed.*, 2010, **49**, 4915–4918; (b) S. Y. Kim, J. Park, M. Koh, S. B. Park and J.-I. Hong, *Chem. Commun.*, 2009, 4735–4737; (c) S. Rochat and K. Severin, *Chem. Commun.*, 2011, **47**, 4391–4393; (d) F. Zheng, F. Zeng, C. Yu, X. Hou and S. Wu, *Chem. – Eur. J.*, 2013, **19**, 936–942; (e) T. Liu, A. Nonat, M. Beyler, M. Regueiro-Figueroa, K. Nchimi Nono, O. Jeannin, F. Camerel, F. Debaene, S. Cianfrani-Sanglier, R. Tripier, C. Platas-Iglesias and L. J. Charbonnière, *Angew. Chem., Int. Ed.*, 2014, **53**, 7259–7263.
- (a) J. F. Zhang, C. S. Lim, S. Bhuniya, B. R. Cho and J. S. Kim, *Org. Lett.*, 2011, **13**, 1190–1193; (b) F. Han, Y. Bao, Z. Yang, T. M. Fyles, J. Zhao, X. Peng, Y. Wu and S. Sun, *Chem. – Eur. J.*, 2007, **13**, 2880–2892; (c) M. Boiocchi, L. Del Boca, D. E. Gómez, L. Fabbrizzi, M. Licchelli and E. Monzani, *J. Am. Chem. Soc.*, 2004, **126**, 16507–16514; (d) M. Vázquez, L. Fabbrizzi, A. Taglietti, R. M. Pedrido, A. M. González-Noya and M. R. Bermejo, *Angew. Chem., Int. Ed.*, 2004, **43**, 1962–1965.
- (a) S. Guha and S. Saha, *J. Am. Chem. Soc.*, 2010, **132**, 17674–17677; (b) X. Cao, W. Lin, Q. Yu and J. Wang, *Org. Lett.*, 2011, **13**, 6098–6101; (c) E. Quinlan, S. E. Matthews and T. Gunnlaugsson, *J. Org. Chem.*, 2007, **72**, 7497–7503.
- S. J. M. Koskela, T. M. Fyles and T. D. James, *Chem. Commun.*, 2005, 945–947.
- (a) X. Jiang, M. C. Vieweger, J. C. Bollinger, B. Dragnea and D. Lee, *Org. Lett.*, 2007, **9**, 3579–3582; (b) C. R. Wade, I.-S. Ke and F. P. Gabbaï, *Angew. Chem.*, 2012, **124**, 493–496.
- (a) Y. Kim and F. P. Gabbaï, *J. Am. Chem. Soc.*, 2009, **131**, 3363–3369; (b) P. Sokkalingam and C.-H. Lee, *J. Org. Chem.*, 2011, **76**, 3820–3828; (c) T. Nishimura, S.-Y. Xu, Y.-B. Jiang, J. S. Fossey, K. Sakurai, S. D. Bull and T. D. James, *Chem. Commun.*, 2013, **49**, 478–480; (d) M. J. Langton, O. A. Blackburn, T. Lang, S. Faulkner and P. D. Beer, *Angew. Chem., Int. Ed.*, 2014, **53**, 11463–11466.
- S. J. Butler and D. Parker, *Chem. Soc. Rev.*, 2013, **42**, 1652–1666.
- (a) R. Pal, D. Parker and L. C. Costello, *Org. Biomol. Chem.*, 2009, **7**, 1525–1528; (b) D. G. Smith, G.-I. Law, B. S. Murray, R. Pal, D. Parker and K.-L. Wong, *Chem. Commun.*, 2011, **47**, 7347–7349; (c) S. J. Butler, B. K. McMahon, R. Pal, D. Parker and J. W. Walton, *Chem. – Eur. J.*, 2013, **19**, 9511–9517.
- L. S. M. P. Lima, A. Lecointre, J.-F. Morfin, A. de Blas, D. Visvikis, L. C. J. Charbonnière, C. Platas-Iglesias and R. Tripier, *Inorg. Chem.*, 2011, **50**, 12508–12521.
- A. Beeby, I. M. Clarkson, R. S. Dickins, S. Faulkner, D. Parker, L. Royle, A. S. de Sousa, J. A. Gareth Williams and M. Woods, *J. Chem. Soc., Perkin Trans. 2*, 1999, 493–504.
- The concentration of  $\text{HCO}_3^-$  in water rises with increased pH. A pH titration revealed that the emission spectral profile of  $[\text{Eu}(\text{L}^1)]^+$  did not change at all within pH range 3.5–7.0 (where the level of  $\text{HCO}_3^-$  is negligible), but was sensitive to the increased amount of  $\text{HCO}_3^-$  present in the pH range 7.1–8.5 (Fig. S3, ESI†).
- Energy minimised structures were determined using the polarised continuum solvent model (PCM), using water as solvent.
- A search of the CCDC database reveals four examples of Ln complexes with a coordinated fluoride ion, and intramolecular  $\text{C}-\text{H}\cdots\text{F}^-$  contacts shorter than 3.1 Å. e.g. A. C. Hillier, X. Zhang, G. H. Maunder, S. Y. Liu, T. A. Eberspacher, M. V. Metz, R. McDonald, Å. Domingos, N. Marques, V. W. Day, A. Sella and J. Takats, *Inorg. Chem.*, 2001, **40**, 5106–5116.
- S. Aime, A. S. Batsanov, M. Botta, J. A. K. Howard, M. P. Lowe and D. Parker, *New J. Chem.*, 1999, **23**, 669–670.

